



Synthesis and crystal structures of four complexes based on Schiff base

Yanpei Song, Kaisheng Diao, Han Xiao & Fang Zhao

To cite this article: Yanpei Song, Kaisheng Diao, Han Xiao & Fang Zhao (2016) Synthesis and crystal structures of four complexes based on Schiff base, Molecular Crystals and Liquid Crystals, 641:1, 39-52, DOI: [10.1080/15421406.2015.1038023](https://doi.org/10.1080/15421406.2015.1038023)

To link to this article: <http://dx.doi.org/10.1080/15421406.2015.1038023>



Published online: 15 Dec 2016.



Submit your article to this journal [↗](#)



Article views: 4



View related articles [↗](#)



View Crossmark data [↗](#)

Synthesis and crystal structures of four complexes based on Schiff base

Yanpei Song^{a,c}, Kaisheng Diao^{a,b}, Han Xiao^a, and Fang Zhao^a

^aCollege of Chemistry and Chemical Engineering, Guangxi University for Nationalities, Nanning, China; ^bGuangxi Key Laboratory of Chemistry and Engineering of Forest Products, Guangxi University for Nationalities, Nanning, China; ^cZhengzhou Xinzheng Meijiu Industrial Co., Ltd., Zhengzhou, China

ABSTRACT



Four new metal–organic complexes of the formula $[\text{CrL}'\text{Cl}_2]$ (1), $[\text{CuL}'\text{Cl}_2]$ (2), $[\text{MnL}''\text{Cl}_2 \cdot \text{H}_2\text{O}]$ (3), and $[\text{NiL}''(\text{OH})_2 \cdot 2\text{NO}_3]$ (4) [$\text{L}' = \text{N}$ -(1-Pyrazin-2-yl-ethylidene)-ethane-1,2-diamine, $\text{L}'' = \text{N}, \text{N}'$ -Bis-(1-pyrazin-2-yl-ethylidene)-ethane-1,2-diamine] have been synthesized and characterized by infrared method, elemental analysis, X-ray powder diffraction analysis, and single-crystal X-ray diffraction techniques. Their heat stability was tested by thermo gravimetric analyzer. X-ray structure analysis reveals that complexes 1–4 are all 0 D structure. The L ligand have many types of coordination modes that make these complexes as having different configuration π – π stackings and/or hydrogen bonding interactions, which seem to be effective in stabilizing these crystal structures.

KEYWORDS

Complex; crystal structure; Schiff base ligand

Introduction

Schiff bases that are ubiquitous in developing intriguing coordination models with transition metals play a crucial role in the development of coordination chemistry because of their preparative accessibility and structural variety [1–3]. These metal complexes based on Schiff base ligands can be widely applied in catalysis, magnetism, and material chemistry [4–6], mainly due to their stability, easy preparation, structural variability, and biological activity [7–10]. Especially, pyrazine-Schiff base ligands containing an additional nitrogen donor in the pyrazine unit can systematically be used to understand the features of supramolecular architectures, and to explore the fascinating properties of these supramolecular frameworks. However, to the best of our knowledge, there are only few studies on the coordination architectures based on pyrazine-Schiff base ligands containing a flexible spacer. Herein, we report the synthesis and structure of four new complexes derived from pyrazine-Schiff base: $[\text{CrL}'\text{Cl}_2]$ (1), $[\text{CuL}'\text{Cl}_2]$ (2), $[\text{MnL}''\text{Cl}_2 \cdot \text{H}_2\text{O}]$ (3), and $[\text{NiL}''(\text{OH})_2 \cdot 2\text{NO}_3]$ (4). In addition, the luminescence activities of L and 1–4 are also described. In supermolecular construction, hydrogen bonding and the π – π stacking interactions are usually very important, which make the structure more stable. The work will contribute to the supermolecular construction of different framework with the same ligands.

CONTACT Kaisheng Diao  dksgxun@hotmail.com  College of Chemistry and Chemical Engineering, Guangxi University for Nationalities, Nanning 530006, China.

CCDC 1041352, 1041353, 1041354, and 1041355 contain the supplementary crystallographic data for this paper. This can be accessed from <http://www.ccdc.cam.ac.uk/conts/retrieving.html>.

Color versions of one or more of the figures in the article can be found online at www.tandfonline.com/gmcl.

© 2016 Taylor & Francis Group, LLC

Table 1. Crystal structure data for complexes 1, 2, 3, and 4.

Compounds	1	2	3	4
Empirical formula	C ₈ H ₁₂ Cl ₂ CrN ₄	C ₈ H ₁₀ Cl ₂ CuN ₄	C ₁₄ H ₁₈ Cl ₂ MnN ₆ O	C ₁₄ H ₁₈ N ₈ NiO ₈
Formula weight	287.12	298.66	412.18	485.07
Temperature (K)	296 (2)	296 (2)	296 (2)	296 (2)
Wavelength	0.71073	0.71073	0.71073	0.71073
Crystal system	Triclinic	Triclinic	Monoclinic	Monoclinic
Space group	<i>P</i> -1	<i>P</i> -1	<i>P</i> 2 (1)/ <i>c</i>	<i>P</i> 2 (1)/ <i>c</i>
<i>a</i> (Å)	6.979 (4)	6.980 (3)	8.318 (2)	13.617 (5)
<i>b</i> (Å)	8.825 (6)	8.829 (3)	7.629 (2)	10.952 (5)
<i>c</i> (Å)	10.208 (2)	10.206 (4)	28.311 (8)	13.453 (5)
α (°)	69.640 (7)	69.660 (4)	90	90
β (°)	72.868 (7)	72.905 (4)	90.261 (4)	96.467 (5)
γ (°)	83.299 (8)	83.255 (4)	90	90
<i>V</i> (Å ³)	563.2 (6)	563.7 (4)	1796.5 (9)	1993.4 (14)
<i>D_c</i> (Mg/m ³)	1.693	1.760	1.524	1.616
<i>Z</i>	2	2	4	4
μ (mm ⁻¹)	1.461	2.382	1.046	1.035
<i>F</i> (000)	292	302	844	1000
Crystal size (mm)	0.32 × 0.31 × 0.30	0.32 × 0.30 × 0.29	0.12 × 0.12 × 0.12	0.21 × 0.21 × 0.20
θ (range)	2.21–24.80	2.21–24.50	1.44–25.00	1.51–25.99
Index (range)	–8 ≤ <i>h</i> ≤ 7 –9 ≤ <i>k</i> ≤ 10 –11 ≤ <i>l</i> ≤ 11	–8 ≤ <i>h</i> ≤ 8 –10 ≤ <i>k</i> ≤ 7 –11 ≤ <i>l</i> ≤ 10	–9 ≤ <i>h</i> ≤ 9 –8 ≤ <i>k</i> ≤ 9 –33 ≤ <i>l</i> ≤ 31	–16 ≤ <i>h</i> ≤ 14 –13 ≤ <i>k</i> ≤ 12 –13 ≤ <i>l</i> ≤ 16
Reflections collected	2938	2939	9443	11,408
Independent reflections	1844 [R (int) = 0.0220]	1845 [R (int) = 0.0167]	3158 [R (int) = 0.0489]	3913 [R (int) = 0.0281]
Completeness to θ = 24.48, 24.50, 25.00, 25.99	0.990	0.988	0.998	0.998
Max. and min. transmission	0.6684 and 0.6521	0.5450 and 0.5161	0.8847 and 0.8847	0.8197 and 0.8119
Data/restraints/parameters	1844/0/137	1845/0/137	3158/1/219	3913/0/284
Goodness of fit on <i>F</i> ²	1.107	1.080	1.068	1.023
<i>R</i> indices [<i>I</i> > 2σ(<i>I</i>)]	<i>R</i> 1 = 0.0608 <i>wR</i> 2 = 0.1835	<i>R</i> 1 = 0.0286, <i>wR</i> 2 = 0.0989	<i>R</i> 1 = 0.0411, <i>wR</i> 2 = 0.1116	<i>R</i> 1 = 0.0451, <i>wR</i> 2 = 0.1283
<i>R</i> indices (all data)	<i>R</i> 1 = 0.0689 <i>wR</i> 2 = 0.1949	<i>R</i> 1 = 0.0315 <i>wR</i> 2 = 0.1081	<i>R</i> 1 = 0.0619 <i>wR</i> 2 = 0.1324	<i>R</i> 1 = 0.0583, <i>wR</i> 2 = 0.1364
Largest diff. features (eÅ ⁻³)	0.789 and –0.851	0.444 and –0.418	0.281 and –0.340	0.517 and –0.497

Table 2. The selected bond lengths (Å) and angles (°) for complexes 1, 2, 3, and 4.

Complex 1			
Cl(2)–Cr (1)	2.471 (2)	N(3)–Cr(1)–Cl (1)	159.13 (19)
Cl(1)–Cr (1)	2.256 (3)	N(4)–Cr(1)–Cl (1)	97.4 (2)
Cr(1)–N (3)	1.973 (6)	N(1)–Cr(1)–Cl (1)	95.96 (18)
Cr(1)–N (4)	2.004 (7)	N(3)–Cr(1)–Cl (2)	99.20 (19)
Cr(1)–N (1)	2.046 (7)	N(4)–Cr(1)–Cl (2)	99.0 (2)
N(3)–Cr(1)–N (4)	82.1 (3)	N(1)–Cr(1)–Cl (2)	97.20 (2)
N(3)–Cr(1)–N (1)	78.6 (2)	Cl(1)–Cr(1)–Cl (2)	101.47 (8)
N(4)–Cr(1)–N (1)	156.5 (3)		
Complex 2			
Cu(1)–N (3)	1.981 (3)	N(3)–Cu(1)–Cl (1)	159.18 (9)
Cu(1)–N (4)	2.008 (3)	N(4)–Cu(1)–Cl (1)	97.76 (10)
Cu(1)–N (1)	2.052 (3)	N(1)–Cu(1)–Cl (1)	96.05 (9)
Cu(1)–Cl (1)	2.2572 (13)	N(3)–Cu(1)–Cl (2)	99.23 (9)
Cu(1)–Cl (2)	2.4710 (12)	N(4)–Cu(1)–Cl (2)	98.73 (11)
N(3)–Cu(1)–N (4)	81.73 (12)	N(1)–Cu(1)–Cl (2)	97.24 (9)
N(3)–Cu(1)–N (1)	78.58 (11)	Cl(1)–Cu(1)–Cl (2)	101.40 (4)
N(4)–Cu(1)–N (1)	156.35 (13)		
Complex 3			
Cl(1)–Mn (1)	2.4316 (12)	N(2)–Mn(1)–N (5)	151.12 (10)
Cl(2)–Mn (1)	2.4333 (12)	N(3)–Mn(1)–Cl (1)	107.95 (9)
Mn(1)–N (3)	2.272 (3)	N(4)–Mn(1)–Cl (1)	120.75 (8)
Mn(1)–N (4)	2.281 (3)	N(2)–Mn(1)–Cl (1)	85.21 (8)
Mn(1)–N (2)	2.379 (3)	N(5)–Mn(1)–Cl (1)	83.28 (8)
Mn(1)–N (5)	2.393 (3)	N(3)–Mn(1)–Cl (2)	111.63 (8)
N(3)–Mn(1)–N (4)	72.45 (10)	N(4)–Mn(1)–Cl (2)	97.91 (8)
N(3)–Mn(1)–N (2)	69.57 (10)	N(2)–Mn(1)–Cl (2)	82.93 (7)
N(4)–Mn(1)–N (2)	139.24 (10)	N(5)–Mn(1)–Cl (2)	84.92 (8)
N(3)–Mn(1)–N (5)	139.29 (10)	Cl(1)–Mn(1)–Cl (2)	131.19 (5)
N(4)–Mn(1)–N (5)	68.45 (10)		
Complex 4			
Ni(1)–N (4)	2.005 (3)	N(4)–Ni(1)–N (5)	77.81 (11)
Ni(1)–N (3)	2.013 (3)	N(3)–Ni(1)–N (5)	159.56 (11)
Ni(1)–O (2)	2.091 (2)	O(2)–Ni(1)–N (5)	86.75 (10)
Ni(1)–O(1)	2.116 (2)	O(1)–Ni(1)–N (5)	86.95 (9)
Ni(1)–N (5)	2.118 (3)	N(4)–Ni(1)–N (2)	159.70 (11)
Ni(1)–N (2)	2.122 (3)	N(3)–Ni(1)–N (2)	77.89 (11)
N(4)–Ni(1)–N (3)	81.93 (12)	O(2)–Ni(1)–N (2)	86.75 (10)
N(4)–Ni(1)–O (2)	96.52 (10)	O(1)–Ni(1)–N (2)	87.92 (10)
N(3)–Ni(1)–O (2)	93.01 (11)	N(5)–Ni(1)–N (2)	122.45 (10)
N(4)–Ni(1)–O (1)	92.25 (11)	O(2)–Ni(1)–O (1)	167.89 (10)
N(3)–Ni(1)–O (1)	96.50 (10)		

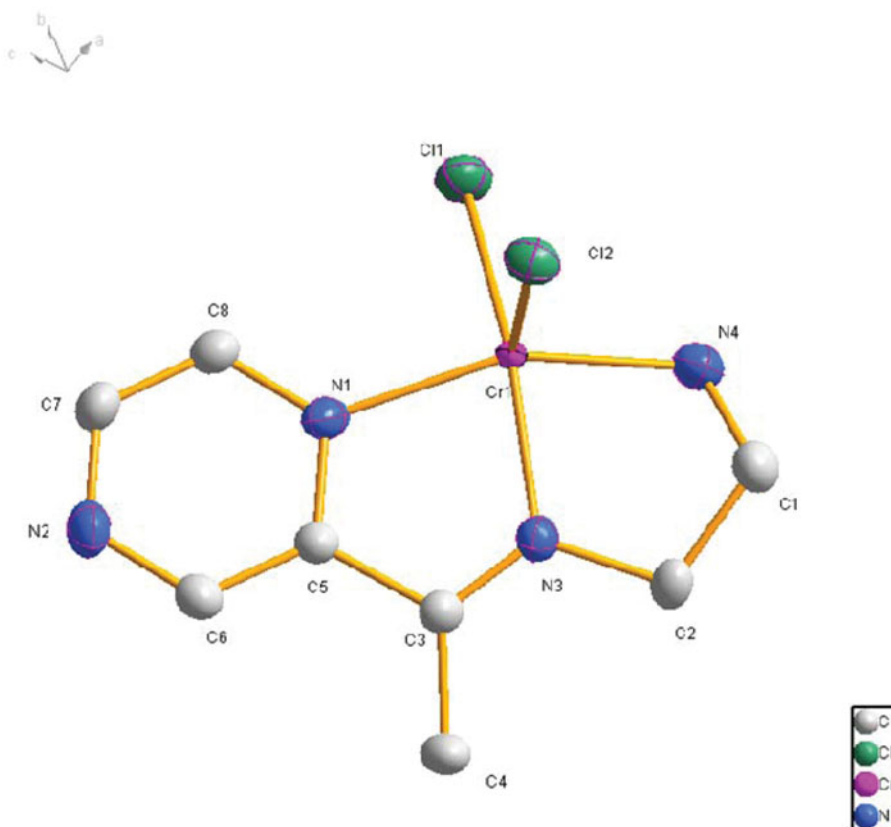
Experimental

Materials and physcial measurements

All reagents and solvents were used directly as supplied commercially without further purification. Elemental analysis for C, H, and N was carried out on a Perkin–Elmer 2400 II elemental analyzer. The FT-IR spectrum was obtained on a FT-IR spectrometer of PE spectrum one in the 4000–400 cm^{−1} regions, using KBr pellets. The X-ray powder diffraction (XRPD) was recorded on an XD-3 diffractometer (Beijing, China) at 36 kV, 25 mA for a Cu-target tube, and a graphite monochromator. Simulation of XRPD spectra was carried out by diffraction-crystal module of the mercury (Hg) program fitting with the single-crystal data. The thermogravimetric analysis (TGA) was performed with a Perkin–Elmer TG=DTA 6300 instrument system at a scan rate of 10°C min^{−1} up to 800°C under protection N₂ flow.

Table 3. Hydrogen bond geometry (Å) of complexes.

D-H ...A	D-H	H ...A	D ...A	<(DHA)	Symmetry codes
Complex 1					
N4-H4D ...Cl1	0.900	2.741	3.4770	140	1-x, 2-y, 1-z
N4-H4E ...Cl2	0.900	2.732	3.4529	138	2-x, 2-y, 1-z
C6-H6 ...Cl2	0.930	2.719	3.6246	165	1-x, 1-y, 2-z
C7-H7 ...Cl2	0.930	2.730	3.6171	160	1-x, 2-y, 2-z
Complex 2					
N4-H4A ...Cl1	0.900	2.746	3.4801	140	1-x, -y, 1-z
N4-H4B ...Cl2	0.900	2.743	3.4638	138	-x, -y, 1-z
C6-H6 ...Cl2	0.930	2.724	3.6311	165	1-x, 1-y, -z
C7-H7 ...Cl2	0.930	2.751	3.6381	160	1-x, -y, -z
Complex 3					
O1-H1D ...Cl1	0.849	2.472	3.3216	179	x, -1+y, z
O1-H1E ...Cl2	0.851	2.432	3.2823	179	
C7-H7A ...N6	0.970	2.601	3.4126	141	1-x, 1-y, -z
C8-H8A ...N1	0.970	2.608	3.5085	154	1-x, -1/2+y, 1/2-z
C10-H10A ...O1	0.960	2.514	3.4006	154	-1+x, y, z
Complex 4					
O1-H1 ...O7	0.820	2.441	3.1312	144	x, 1/2-y, -1/2+z
O1-H1 ...O8	0.820	2.077	2.8616	162	
O2-H2 ...O5	0.820	2.128	2.8853	155	x, 1/2-y, -1/2+z
C2-H2A ...O3	0.929	2.489	3.3375	153	-1+x, y, z
C8-H8A ...O4	0.969	2.560	3.3148	135	1-x, 1-y, -z
C10-H10B ...O7	0.960	2.530	3.3662	145	x, 1+y, z
C13-H13 ...O8	0.930	2.436	3.1916	137	-x, 1/2+y, 1/2-z

**Figure 1.** The coordination environment of complex 1. Thermal ellipsoids are shown at 30% probability, all H atoms are omitted for clarity.

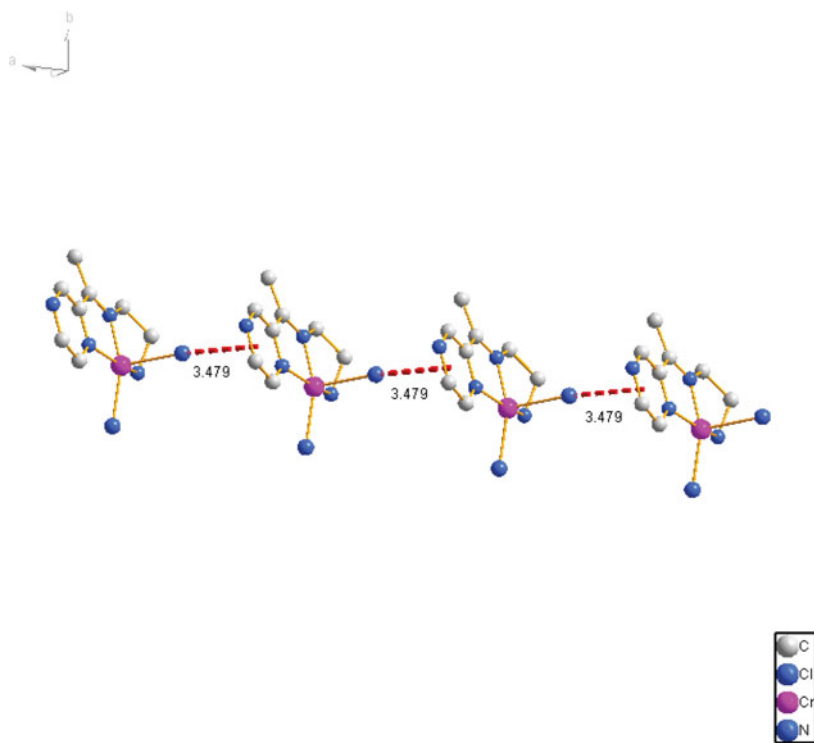


Figure 2. Weak Cr-Cl... π interaction in complex 1.

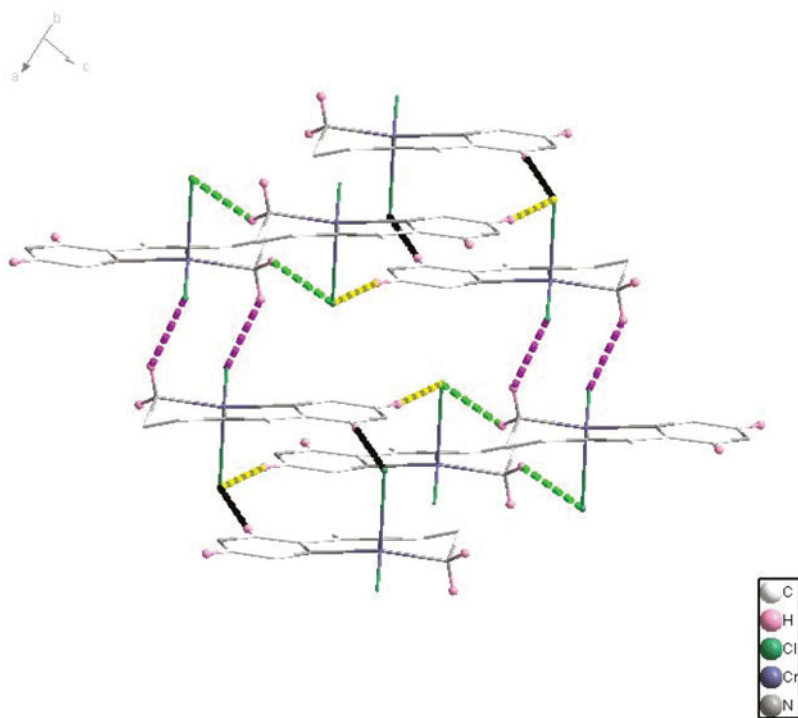


Figure 3. Weak N-H...Cl and C-H...Cl interaction in complex 1.

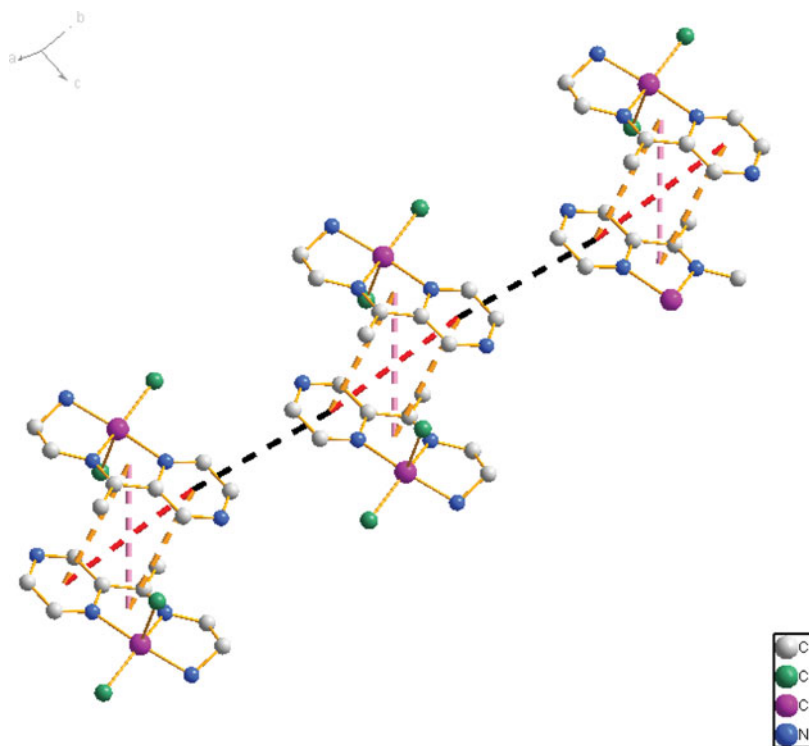


Figure 4. Weak $\pi-\pi$ interaction in complex 1.

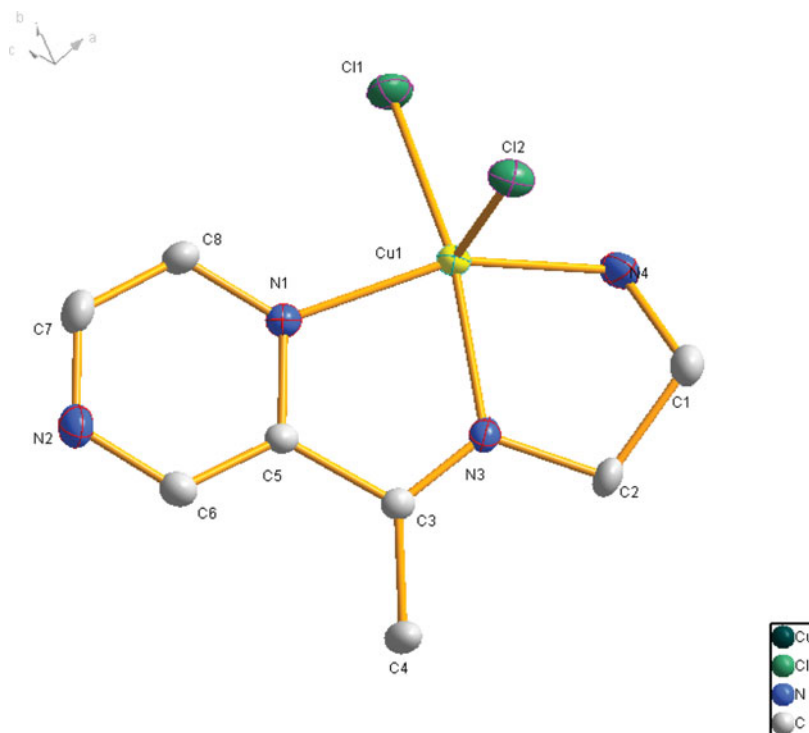


Figure 5. The coordination environment of complex 2. Thermal ellipsoids are shown at 30% probability, all H atoms are omitted for clarity.

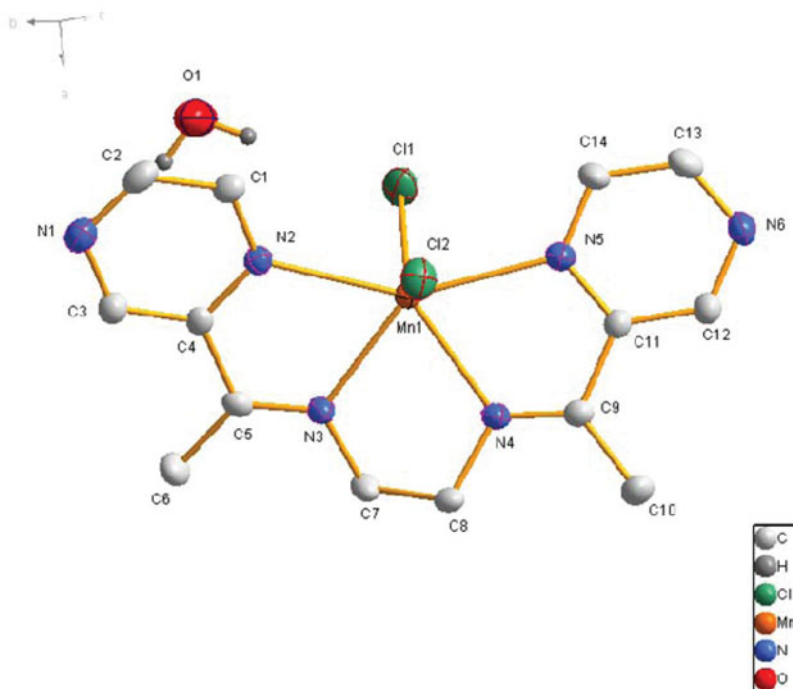


Figure 6. The coordination environment of complex 3. Thermal ellipsoids are shown at 30% probability, all H atoms are omitted for clarity.

Synthesis of $C_8H_{12}Cl_2CrN_4$ (1)

An acetonitrile solution of L' (0.1 mmol, 0.0164 g) was added to $CrCl_3 \cdot 6H_2O$ (0.1 mmol, 0.0414 g) with constant stirring. After 5 min, the reaction solution was filtered to remove a small quantity of precipitation. Kept for the slow evaporation of filtrate at room temperature, X-ray quality luminous block-shaped single crystals were obtained in 6 h. The crystals were isolated, washed with acetonitrile, and dried in a vacuum drying chamber. Yield, 92%. Anal. Calc. for $C_8H_{12}Cl_2CrN_4$ (287.12): C, 33.48; H, 4.21; N, 19.52. Found: C, 33.56; H, 4.18; N, 19.59%. Selected IR data (cm^{-1}): 3437 (w), 3289 (s), 3234 (s), 3082 (w), 3032 (w), 3008 (w), 1658 (s), 1564 (m), 1471 (w), 1411 (s), 1373 (w), 1182 (m), 1108 (m), 1040 (s), 865 (w), 659 (w).

Synthesis of $C_8H_{12}Cl_2CuN_4$ (2)

Complex 2 was synthesized by a method similar to that for Complex 1, except with the use of $CuCl_2 \cdot 2H_2O$ instead of $CrCl_3 \cdot 6H_2O$. Peacock green crystals suitable for X-ray analysis were obtained within 6 h. Yield: 84.62%. Anal. Calc. for $C_8H_{12}Cl_2CuN_4$ (298.66): C, 32.19; H, 4.05; N, 18.76. Found: C, 32.28; H, 4.13; N, 18.75%. Selected IR data (cm^{-1}): 3445 (w), 3289 (s), 3235 (m), 3082 (w), 3033 (w), 3008 (w), 2975 (w), 1658 (s), 1564 (m), 1411 (s), 1373 (m), 1302 (w), 1183 (s), 1109 (m), 1041 (s), 865 (w), 661 (w).

Synthesis of $C_{14}H_{18}Cl_2MnN_6O$ (3)

To a hot stirring solution of ligand L'' (0.1 mmol, 0.0268 g) in 15-mL acetone, $MnCl_2 \cdot 4H_2O$ (0.1 mmol, 0.0198 g) in 10-mL acetone was added dropwise and the mixture was stirred for



Figure 7. Weak O-H ...Cl, C-H ...N, and C-H ...O interaction in complex 1.

5 min. Brilliant yellow crystals suitable for X-ray analysis were obtained by slow evaporation of the filtrate at room temperature. Yield: 79.16%. Anal. Calc. for $C_{14}H_{18}Cl_2MnN_6O$ (412.18): C, 40.86; H, 4.40; N, 20.39. Found: C, 40.89; H, 4.44; N, 20.45%. Selected IR data (cm^{-1}): 3524 (s), 3464 (s), 2919 (w), 1643 (s), 1431 (w), 1407 (m), 1383 (m), 1310 (m), 1172 (s), 1136 (w), 1030 (s), 858 (w), 516 (w).

Synthesis of $C_{14}H_{18}N_8NiO_8$ (4)

Complex 4 was synthesized by a method similar to that for Complex 3, except with the use of $Ni(NO_3)_2 \cdot 6H_2O$ instead of $MnCl_2 \cdot 4H_2O$. Brown single crystals suitable for X-ray analysis were obtained within 8 h. Yield: 82.92%. Anal. Calc. for $C_{14}H_{18}N_8NiO_8$ (485.07): C, 34.68; H, 3.74; N, 23.11. Found: C, 34.75; H, 3.78; N, 23.21. Selected IR data (cm^{-1}): 3255 (s), 1667 (m), 1384 (s), 1333 (m), 1176 (m), 1036 (m), 867 (w), 830 (w).

Single-crystal structure determination and refinement

Crystallographic data of complexes were collected on a Bruker SMART CCD diffractometer with graphite monochromated Mo-K α radiation ($\lambda = 0.71073 \text{ \AA}$) at $T = 296 \text{ K}$. Absorption corrections were applied by using the multi-scan program [11]. The structure was solved by direct methods and successive Fourier difference syntheses (SHELXS-97), and anisotropic thermal parameters for all non-hydrogen atoms were refined by full-matrix least-squares procedure against F^2 (SHELXL-97) [12]. All non-hydrogen atoms were refined anisotropically.

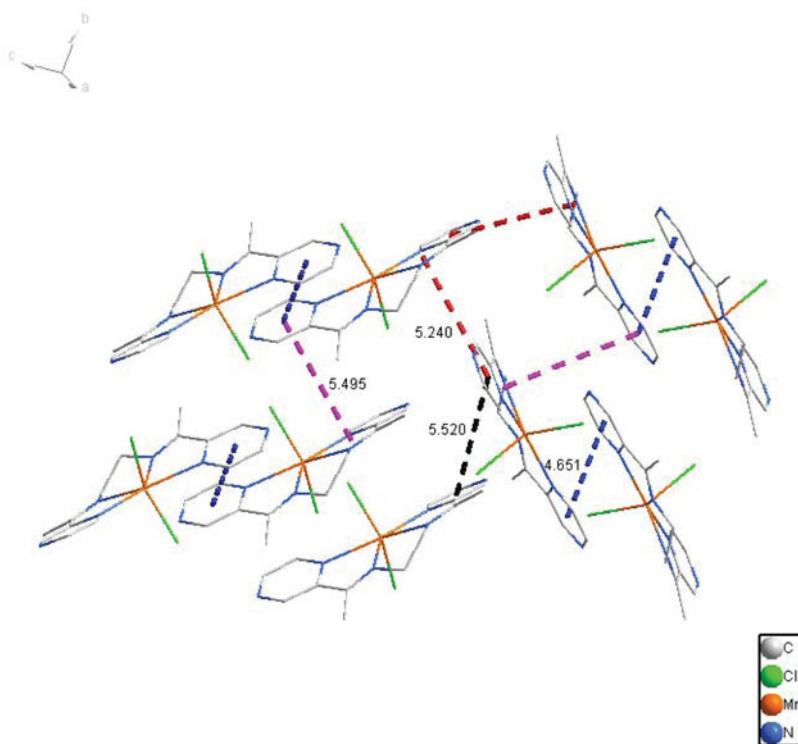


Figure 8. Weak π – π interaction in complex 3.

Hydrogen atoms were set in calculated positions and refined in a riding mode with a common thermal parameter. All hydrogens were absent expect that they alter their occupancy to get the correct formula. The crystallographic data and experimental details for the structure analysis are summarized in Table 1, the selected bond lengths and angles are listed in Table 2, and the hydrogen-bonds of these complexes are listed in Table 3.

Results and discussions

Crystal structure descriptions

Complex 1 is a mononuclear, five-coordinate species. The central Cr ion is coordinated by two chloride and three N atoms. The Schiff base (L') acts as a tridentate chelating ligand, giving two five-membered rings and displays a distorted square-pyramidal geometry with the apical position occupied by a Cl atom. The molecular structure of Complex 1 is shown in Fig. 1. Atoms N1, N2, N3, and Cl2 form the basal plane and atom Cl is in apical position. The effect of the chelate rings is clearly observed in the N3–Cr1–N4 and N3–Cr1–N1 bond angles, which deviate by 7.9° and 11.4° , respectively, from the ideal value (90°). As a result, the N(4)–Cr(1)–N(1) axis is not linear [$156.5(3)^\circ$], significantly deviated from the ideal value of 180° . The Cr–N distances in the basal plane are 2.009 (7), 1.974 (6), and 2.050 Å (6). In the crystal packing, Fig. 2 shows the mode with weak Cr1–Cl2 ...Cg3 (Cl2 to the centroid of ring Cg3: 3.479 Å) interactions. Figure 3 showed that N–H ...Cl hydrogen bonds and C–H ...Cl link the molecules into sheets, which interact weakly to form a 3D framework. figure 4 showed the π – π stacking interactions. The centroid-to-centroid distances of π – π stacking interactions among the five-number rings is 4.813 Å, and between the pyrazine rings and the

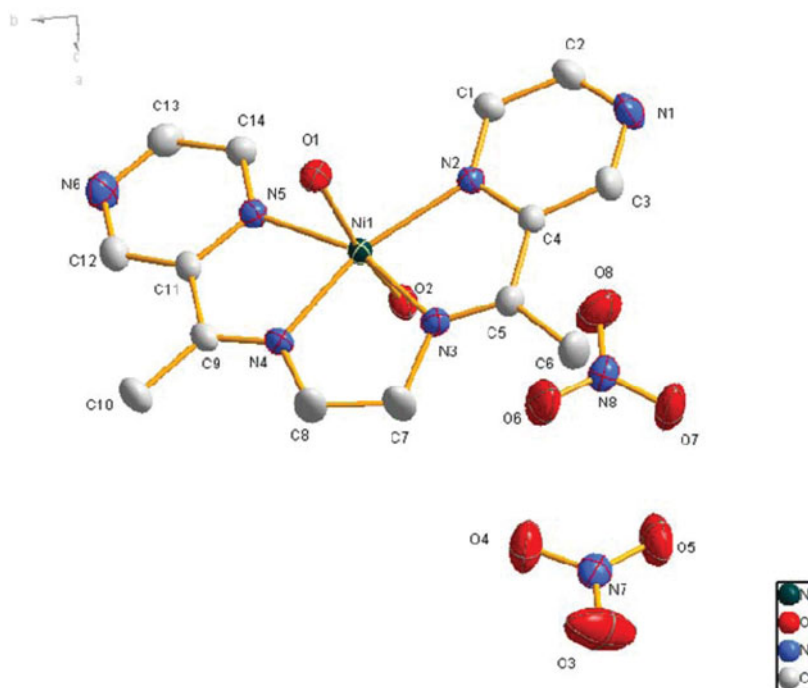


Figure 9. The coordination environment of complex 4. Thermal ellipsoids are shown at 30% probability, all H atoms are omitted for clarity.

five-number rings is 4.526 Å. In addition, the π – π stacking interactions also exist between two pyrazine rings of L' ligands from adjacent layers (5.322, 5.304 Å), which make the structure more stable.

Complex 2 has the same structure as Complex 1, except that the central ion uses Cu instead of Cr. The molecular structure of Complex 2 is shown in Fig. 5. It has the same intermolecular forces as that of Complex 1.

Single crystal X-ray analysis of 3 reveals that the asymmetric unit comprises one Mn(II) ion, one L'' ligand, two Cl^- anions, and one H_2O . The Mn(II) atom in Complex 3 is six coordinate and it coordinates with four nitrogen atoms from ligand L'' and two Cl^- ions. The molecular structure of Complex 3 is shown in Fig. 6. The Mn(1), N(3), N(4), C(7), and C(8) atoms occupy the equatorial plane, while the Cl(1) and Cl(2) atoms occupy the apical positions. The bond distances of Mn(1)–N(3), Mn(1)–N(4) (2.272 (3), 2.281 (3)) is shorter than that of Mn(1)–N(2), Mn(1)–N(5) (2.379 (3), 2.393 (3)) because the coordination ability of the aliphatic N atom is stronger than that of aromatic. The two five-membered coordinated ring, (Mn(1), N(2), N(3), C(4), C(5) and Mn(1), N(4), N(5), C(9), C(11)) is at the opposite position, and their dihedral angle is 20.47°. Three types of hydrogen bonds exist in the complex, which are O–H...Cl, C–H...N, and C–H...O. These molecular hydrogen bonds connect the neighboring molecules to form a three-dimensional (3D) structure (Fig. 7). Fixing of H_2O between layers decreases the total energy of this system and forms the steadiest molecular structure. At the same time, the π – π stacking interactions enhance these connections (Fig. 8).

The structure of Complex 4 is shown in Fig. 9. The structure is clearly a mononuclear six-coordinated species, in which the central Ni(II) is coordinated by four N atoms (N2, N3, N4, and N5) from one chelating molecule of L'' and two coordinate H_2O (O7 and O8), while two

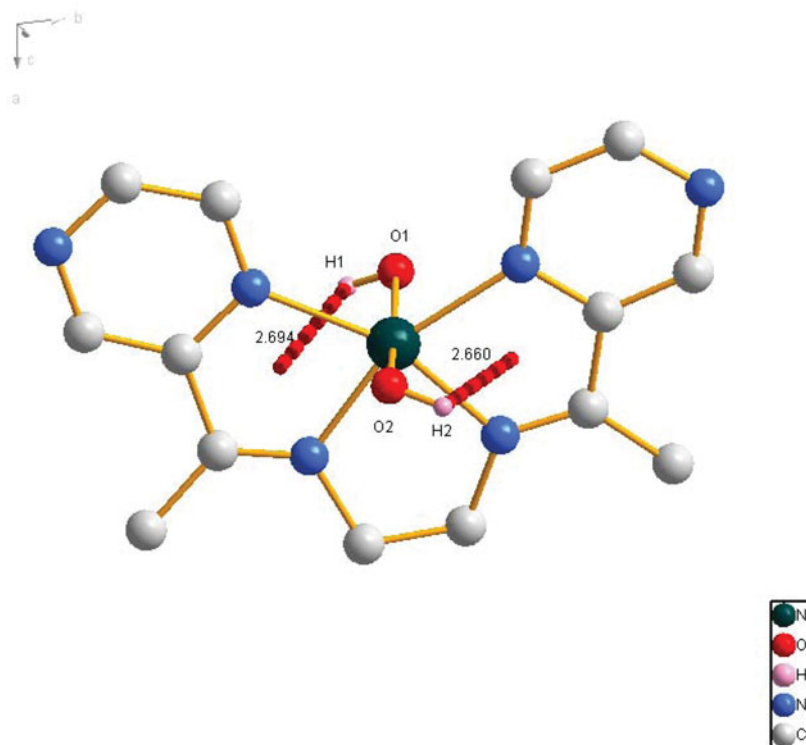


Figure 10. Weak O–H ... π interaction in complex 4.

nitrate anions are free. Two H_2O molecules that coordinate with the center Ni(II) ion link the other molecules to a 3D layer according to O1–H1 ...O7, O1–H1 ...O8, and O2–H2 ...O5 hydrogen bonds. The Ni(1)–O(1), Ni(1)–O(2) bond distances are 2.116 (2), 2.091 (2) respectively. The dihedral angle between two five-membered coordinated ring (Ni(1), N(2), N(3), C(4), C(5) and Ni(1), N(4), N(5), C(9), C(11)) is only 4.62° , and is smaller than that of Complex 3. It has a certain value in the aspect of material design. Figure 10 shows the mode with weak O–H ...Cg (H1 to the centroid of ring Cg1: 2.694 Å, H2 to the centroid of ring Cg3: 2.660 Å) interactions. Figure 11 shows the linkage of nitrate anion with weak N–O ...Cg. Figure 12 shows that O–H ...O hydrogen bonds and C–H ...O link the molecules into sheets and 3D framework. In addition, the nitrate anions also play a connecting role in different molecules of the complex. All these interactions are responsible for the formation of a 3D network in the solid state.

Infrared spectroscopy

The structures of 1–4, L' and L'' ligands were characterized by IR spectra, which showed valuable information about counterions in their respective coordination environments. In the IR spectra, the $\text{C}=\text{N}$ stretching vibrations of free L' and L'' ligands at 1630 cm^{-1} are shifted to 1658, 1655, 1643, and 1667 cm^{-1} of complexes 1–4, which indicate that the $\text{C}=\text{N}$ group is involved in the coordination. The spectrum of 4 reveals strong bands at 1384, 1333, and 1176 cm^{-1} , suggesting that there are nitrate groups in this complex.

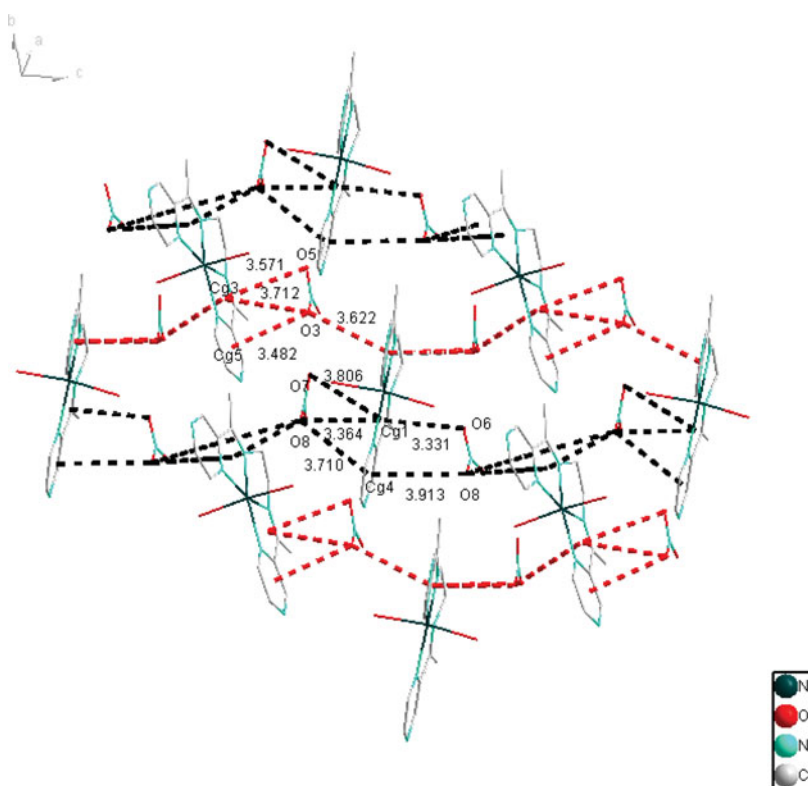


Figure 11. Weak N–O ... π interaction in complex 4.

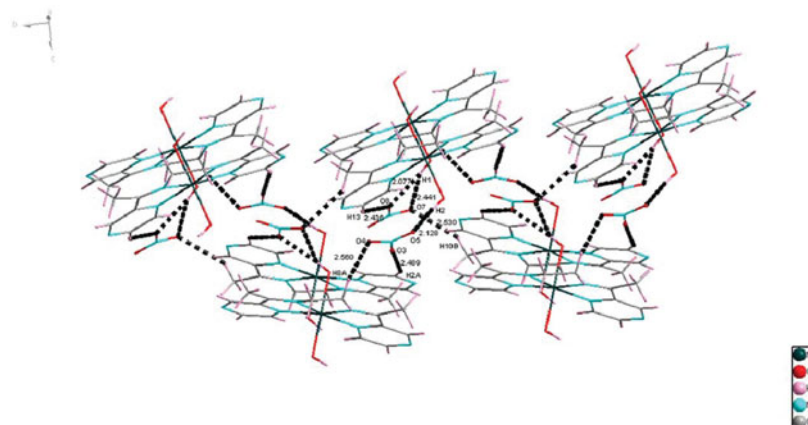


Figure 12. Weak O–H ...O and C–H ...O interactions in complex 4.

X-ray powder diffraction analysis

The structural consistency and phase purity of complexes 1, 2, 3, and 4 were confirmed by comparing the measured pattern calculated from single-crystal data with the experimental XRPD analysis at room temperature (Fig. 13).

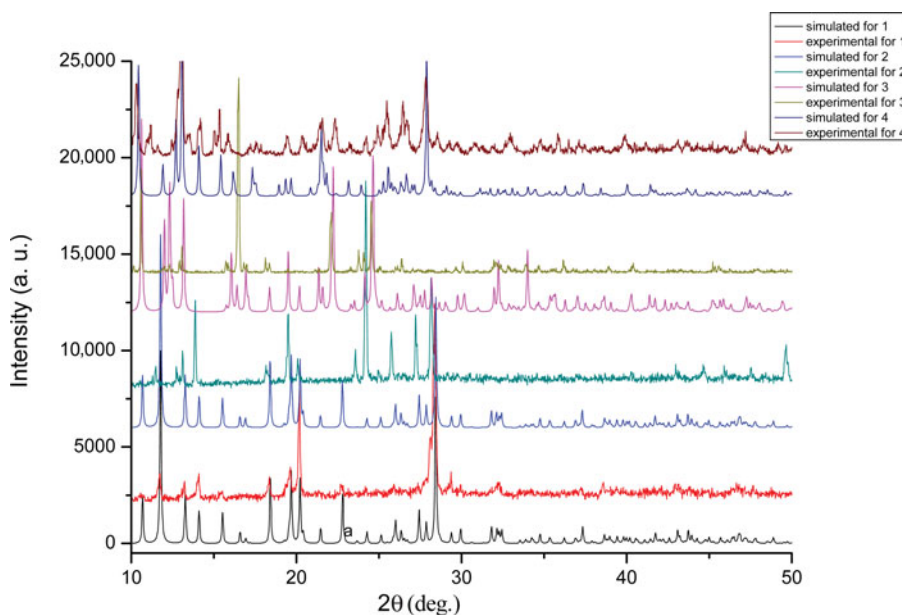


Figure 13. Simulated and experimental XRPD patterns for complexes.

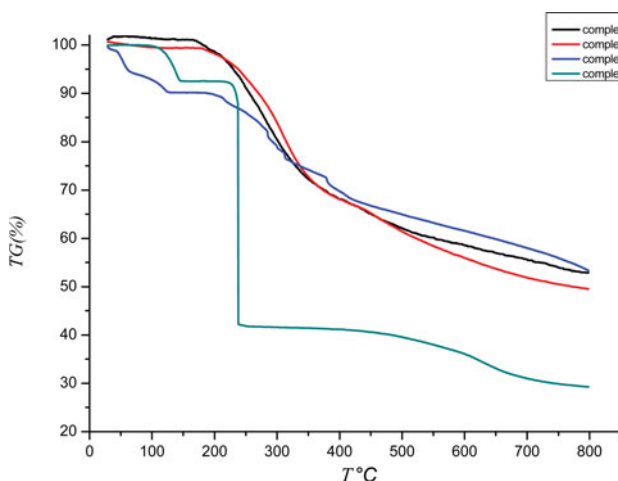


Figure 14. TGA diagrams of complexes 1, 2, 3, and 4.

Thermo gravimetric analyzer analysis

To examine the thermal stability of complexes $[\text{CrL}/\text{Cl}_2]$ (1), $[\text{CuL}/\text{Cl}_2]$ (2), $[\text{MnL}''\text{Cl}_2 \cdot \text{H}_2\text{O}]$ (3), and $[\text{NiL}''(\text{OH})_2 \cdot 2\text{NO}_3]$ (4), thermal gravimetry (TG) was carried out between 28°C and 800°C under nitrogen flow (Fig. 14). For Complex 1, two stages are included in the pyrolysis process. The first stage is from the starting temperature to 170°C, in which a slight weight loss occurs. The second stage, from 170°C to the end, is characterized by a major loss, which relates to the main decomposition process. The TG curves of Complex 2 show similar steps as that with Complex 1 due to their similar frame structure. For Complex 3, the first mass loss value (4.1%) in 60–123°C can be associated with the elimination of free H_2O , which is consistent with that of mass loss calculations (4.3%). Then, heat up to 800, and L'' ligand is decomposed. For Complex 4, the first mass loss value (7.1%) in 70–150°C can be associated

with the elimination of H_2O (dehydration), which is consistent with that of mass loss calculations (7.0%). Then, heat up to 210°C , the free NO_3 and part of ligand are decomposed. It proceeds at a moderate rate in the range 200 to 700°C but holds a comparatively steady rate in the higher range from 700 to 800°C , implying the formation of NiO .

Conclusions

Complexes $[\text{CrL}'\text{Cl}_2]$ (1), $[\text{CuL}'\text{Cl}_2]$ (2), $[\text{MnL}''\text{Cl}_2\cdot\text{H}_2\text{O}]$ (3), and $[\text{NiL}''(\text{OH})_2\cdot 2\text{NO}_3]$ (4) were synthesized, and their structures were characterized by IR method, elemental analysis, XRPD analysis, and single-crystal X-ray diffraction techniques. Their heat stability was analyzed by thermo gravimetric analyzer. The successful preparation of the complexes manifests that the conformations and functions of $\pi-\pi$ stacking interactions, hydrogen bonds, and van der Waals' forces are important factors in influencing the architecture of metal-L ligand complexes.

Funding

Thanks for the support of the Chinese Natural Science Foundation (No.21567004), and the Guangxi Provincial Natural Science Foundation (No. 2013GXNSFAA019091).

References

- [1] Drew, M. G. B., Foreman, M. R. StJ., Hudson, M. J., & Kennedy, K. F. (2004). *Inorg. Chim. Acta*, 357, 4102.
- [2] Liu, J. C., Li, M., Omer, A. S. M., Wei, Y., & Guo, G. Z. (2011). *Acta Cryst. E*, 67, 1555.
- [3] Tan, X. J., Liu, H. Z., Ye, C. Z., Lou, J. F., Liu, Y., Xing, D. X., Li, S. P., Liu, S. L., & Song, L. Z. (2014). *Polyhedron*, 71, 119.
- [4] Hashemi, L., & Morsali, A. (2011). *J. Coord. Chem.*, 64, 4088.
- [5] Louloudi, M., Nastopoulos, V., Gourbatsis, S., Perlepes, S. P., & Hadjiliadis, N. (1999). *Inorg. Chem. Commun.*, 2, 479.
- [6] Wang, W., Zhang, F. X., Li, J., & Zhang, R. L. (2010). *Russ. J. Coord. Chem.*, 36, 378.
- [7] Omer, A. S. M., Liu, J. C., Deng, W. T., & Jin, N. Z. (2014). *Polyhedron*, 69, 10.
- [8] Gourbatsis, S., & Hadjiliadis, N. (1998). *Transition Met. Chem.*, 23, 599.
- [9] Desai, S. B., Desai, P. B., & Desai, K. R. (2001). *Heterocyclic Comm.*, 7, 83.
- [10] Abry, N. M., Lefel, E. M., L-Omar, M. A., & Amr, A., El-Galil E. (2013). *J. Chem.*, 2013, 1.
- [11] Blessing, R. H. (1995). *Acta Crystallogr. A*, 51, 33.
- [12] Sheldrick, G. M. (1997). *SHELXTL97: Program for Refining Crystal Structure Refinement*. University of Göttingen: Göttingen, Germany.